Influence of Doped Anions on Poly(3,4-ethylenedioxythiophene) as Hole Conductors for Iodine–Free Solid–State Dye–Sensitized Solar Cells

ARTICLE *in* JOURNAL OF THE AMERICAN CHEMICAL SOCIETY · FEBRUARY 2008

Impact Factor: 12.11 · DOI: 10.1021/ja075704o · Source: PubMed

J|A|C|S
ARTICLES
Published on Web 01/03/2008

Influence of Doped Anions on Poly(3,4-ethylenedioxythiophene) as Hole Conductors for Iodine-Free Solid-State Dye-Sensitized Solar Cells

Jiangbin Xia,[†] Naruhiko Masaki,[†] Monica Lira-Cantu,[‡] Yukyeong Kim,[†] Kejian Jiang,[†] and Shozo Yanagida*[,†]

Center for Advanced Science and Innovation, Osaka University, Suita, Osaka 565-0871, Japan, and Institut de Ciència de Materials de Barcelona, Campus UAB, Bellaterra E-08193, Spain

Received July 31, 2007; E-mail: yanagida@mls.eng.osaka-u.ac.jp

Abstract: Poly(3,4-ethylenedioxythiophene) (PEDOT) is an excellent hole-conducting polymer able to replace the liquid I^-/I_3^- redox electrolyte in dye-sensitized solar cells (DSCs). In this work we applied the in situ photoelectropolymerization technique to synthesize PEDOT and carried out a careful analysis of the effect of different doping anions on overall solar cell performance. The anions analyzed in this work are ClO_4^-, $CF_3SO_3^-$, BF_4^-, and $TFSI^-$. The best solar cell performance was observed when the $TFSI^-$ anion was used. Photoelectrochemical and impedance studies reveal that the doped anions in the PEDOT hole conductor system have great influences on *I*−*V* curves, conductivity, and impedance. The optimization of these parameters allowed us to obtain an iodine-free solid-state DSC with a maximum J_{sc} of 5.3 mA/cm^2, V_{oc} of 750 mV, and a conversion efficiency of 2.85% which is the highest efficiency obtained so far for an iodine-free solid-state DSC using PEDOT as hole-transport material.

1. Introduction

Since the discovery of nanocrystalline dye sensitized solar cell (DSC) back in 1991,[1] great efforts have been taken in order to improve the performance of the DSC. The fabrication of large-area modules along with their long-term stability tests is currently a reality and demonstrates the research efforts taken to empower this technology. However, several technological challenges must be overcome before DSC can reach large-scale production. The most important issues are related to the application of liquid electrolytes that present solvent evaporation, corrosion of cell components by iodine, or the need for cell sealing.

The substitution of the liquid electrolyte in DSC by solid or semisolid (gel) hole conductor materials have led to what is call as the solid-state dye-sensitized solar cell (ss-DSC). For example, the application of a kind of p-type *inorganic* semiconductor of a Cu(I)-based compound such as CuI or CuSCN[2−3] has shown the existence of imidazolium thiocyanate, a crystal inhibitor which can improve the cells' stability.[4] Moreover, the most promising results so far are related to the application of 2,2′,7,7′-tetrakis(*N*,*N*-di-*p*-methoxyphenyl-amine)9,9′-spirobifluorene (spiro-OMeTAD) reported by the group of Grätzel and, later, by the group of Thelakkat.[5−7] Some results by these groups show the application of spiro-OMeTAD together with the use of Li salts as additives to increase conductivity[8] and demonstrate the improvement of the cell conductivity up to 4% efficiency.[9] Another possibility is the application of p-type *organic* semiconductors such as conducting organic polymers polypyrrole,[10] polyaniline,[11] polydiacetylenes,[12] or poly(3-octylthiopehene).[13−14] The first reports from our group in 1997 showed the possibility of using polypyrrole[10] as hole conductor, although higher efficiencies were required. In an effort to enhance iodine-free ss-DSC efficiency, we developed a new technique called in situ photoelectropolymerization (PEP) where a careful design of the dye properties and the strategically selected monomer oxidation potential was taken into consideration as already described.[15] For this purpose, the monomer 2,2′-bis(3,4-ethylenedioxythiophene) (bis-EDOT) was employed in order to form the

[†] Center for Advanced Science and Innovation, Osaka University.
[‡] Institut de Ciència de Materials de Barcelona.

(1) O'Regan, B.; Grätzel, M. *Nature* **1991**, *353*, 737.
(2) Tennakone, K.; Kumara, G. R. A.; Kottegoda, I. R. M.; Wijayantha, K. G. U.; Perera, V. P. S. *J. Phys. D: Appl. Phys.* **1998**, *31*, 1492.
(3) O'Regan, B.; Schwartz, D. T.; Zakeeruddin, S. M.; Grätzel, M. *Adv. Mater.* **2000**, *12*, 1263.
(4) Kumara, G. R. A.; Konno, A.; Shiratsuchi, K.; Tsukahara, J.; Tennakone, K. *Chem. Mater*. **2002**, *14*, 954.
(5) Bach, U.; Lupo, D.; Comte, P.; Moser, J. E.; Weissörtel, F.; Salbeck, J.; Spreitzer, H.; Grätzel, M. *Nature* **1998**, *395*, 583.
(6) Krüger, J.; Plass, R.; Grätzel, M.; Matthieu, H. J. *Appl. Phys. Lett.* **2002**, *81*, 367.
(7) Peter, K.; Wietasch, H.; Peng, B.; Thelakkat, M. *Appl. Phys. A* **2004**, *79*, 65.
(8) Snaith, H. J.; Grätzel, M. *Appl. Phys. Lett.* **2006**, *89*, 262114.
(9) Schmidt-Mende, L.; Zakeeruddin, S. M.; Grätzel, M. *Appl. Phys. Lett.* **2005**, *86*, 013504.
(10) Murakoshi, K.; Kogure, R.; Wada, Y.; Yanagida, S. *Chem. Lett*. **1997**, *26*, 471.
(11) Tan, X.; Zhai, J.; Wan, M. X.; Meng, Q. B.; Li, Y. L.; Jiang, L.; Zhu, D. B. *J. Phys. Chem. B* **2004**, *108*, 18693.
(12) Wang, Y. P.; Yang, K.; Kim, S. C.; Nagarajan, R.; Samuelson, L. A.; Kumar, J. *Chem. Mater*. **2006**, *18*, 4215.
(13) Gebeyehu, D.; Brabec, C. J.; Sariciftci, N. S. *Thin Solid Films* **2002**, *403*−*404*, 271.
(14) Lancelle-Beltran, E.; Prené, P.; Boscher, C.; Belleville, P.; Buvat, P.; Sanchez, C. *Adv. Mater*. **2006**, *18*, 2579.
(15) Saito, Y.; Fukuri, N.; Senadeera, G. K. R.; Kitamura, T.; Wada, Y.; Yanagida, S. *Electrochem. Commun.* **2004**, *6*, 71.

10.1021/ja075704o CCC: $40.75

Scheme 1. Chemical Structures of (a) Bis-EDOT, PEDOT, and (b) Counter Anions of ClO_4^-, BF_4^-, $CF_3SO_3^-$, and $TFSI^-$

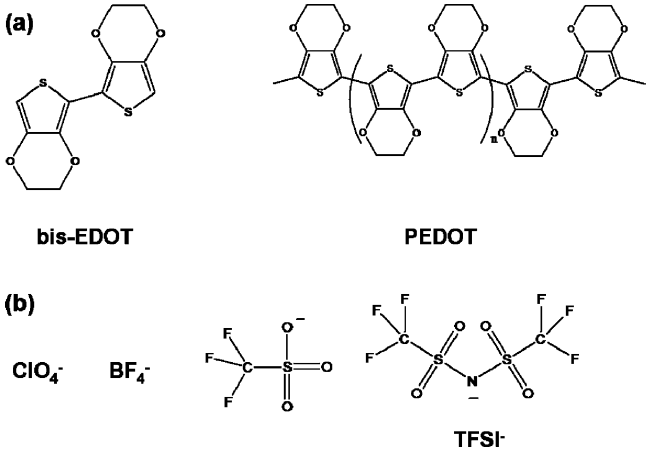

conductive polymer poly(3,4-ethylenedioxythiophene) (PEDOT) by photoelectrochemical oxidation.[15−17] Promising results in our group demonstrated a 2% iodine-free ss-DSC efficiency by the application of the PEP technique together with the use of a novel hybrid Ru complex dye (HRS-1).[18]

On the other hand, several methods have been used for its synthesis, for example electrochemical techniques under aqueous or nonaqueous solution, in the latter case by applying different counteranions within the electrolyte, such as BF_4^-, PSS^-, etc.[19−20] In this work we show the optimization of a simple electrochemical synthesis technique that improves the hole conductivity of PEDOT. We investigated the in situ photoelectropolymerization processes and support our results with the aim of electrochemical impedance spectroscopy (EIS) analysis. Our experiments were carried out in nonaqueous electrolytes and demonstrate that a careful selection of the doping anions and the use of their lithium salts effectively improve overall cell efficiency.

2. Experimental Section

2,2′-bis (3,4-ethylenedioxythiophene) (bis-EDOT) dimer was purchased from Azima company. $LiCF_3SO_3$ and $LiBF_4$ were purchased from Aldrich. Lithium bis-trifluoromethanesulfonylimide (LiTFSI) was purchased from TCI. $LiClO_4$ and other common reagents and organic solvents were purchased from Wako. The chemical structures of bis-EDOT, PEDOT, and different counteranions are shown in Scheme 1.

TiO_2 compact layer or blocking layer was prepared according to a previous report.[15] Nanoporous TiO_2 electrodes were prepared on a FTO (Nippon Sheet Glass, SnO_2:F, 10 ohm/sq) from the colloidal Nanoxide-T paste (Solaronix) by doctor-blade techniques. The films were annealed at 450 °C for 30 min in air. The resulting TiO_2 films (thickness is around 5.5 μm, measured by a profiler, Sloan, Dektak3) were cut into pieces. Then, the electrodes were immersed into 3.0×10^{-4} M *cis*-bis(isothiocyanato)(2,2′-bipyridyl-4,4′-dicarboxylato)(2,2′-bipyridyl-4,4′-di-nonyl)ruthenium(II) (known as Z-907, Solaronix) in acetonitrile/*tert*-butanol (1:1) for 18 h.

Acetonitrile solutions of 0.1 M $LiClO_4$, $LiBF_4$, LiTFSI, and $LiCF_3SO_3$ were prepared before use. The dyed TiO_2 film as a working electrode, a platinum foil as a counterelectrode, and Ag/AgCl as a reference electrode (BAS 100B/W electrochemical system) were employed. A concentration of 0.01 M bis-EDOT in supporting electrolyte was used for the photoelectropolymerization. The photoelectropolymerization was achieved by using the constant potential (+0.2 V vs Ag/AgCl) under light irradiation of a 500 W Xe lamp (22 mW cm^{-2}, $\lambda > 520$ nm) for 30 min. The sheet resistances of the different PEDOT hole conductors were measured by MITSUBISHI KAGAKU MCP-T 600 four-probe-type resistance meter. After in situ photoelectropolymerization, the resulting TiO_2/dye/PEDOT electrode was rinsed by ethanol and then dried. After that, 1 drop of 1-buthyl-3-methyimidazolium bis-trifluoromethansulfonylimide (BMIIm-TFSI) with 0.2 M of 4-*tert*-butylpyridine (TBP) and 0.2 M of LiTFSI was added on the surface. The sandwich-type devices were finished by clipping a counter electrode of FTO/Au. Typical areas of the electrodes were around 0.30 cm^2. The photoelectrochemical properties of the DSCs were studied by recording the current−voltage ($I-V$) characteristics of the unsealed type cell under illumination of AM1.5 (1 Sun; 100 mW/cm^2) by using a solar simulator (Yamashita Denso, YSS-80). The data were obtained from the average of at least three examples. The shunt resistance R_{sh} and series resistance R_s were estimated by the software automatically (PV Tester, version 1.2.3, Yamashita Denso). The calculation should be according to the equation:[21]

$$I = I_{ph} - I_0\left\{\exp\left(q\frac{V + IR_s}{nKT}\right) - 1\right\} - \frac{V + IR_s}{R_{sh}} \qquad (1)$$

where I_0 is initial current, R_s is series resistance, R_{sh} is shunt resistance, n is diode factor, and q, k, T are constants. The R_s value was evaluated from the plot δV vs I at high V part while R_{sh} value was evaluated from the plot of δI vs V at low V part.

The incident photon-to-current conversion efficiency (IPCE) was measured by using a commercial setup for IPCE measurements (PV-25DYE, JASCO) under 5 mW cm^{-2} monochromic light illumination. The EIS of all TiO_2/dye/PEDOT/Au cells were measured with an impedance analyzer (Solartron Analytical, 1260) connected with a potentiostat (Solartron Analytical, 1287) under dark conditions (applied potential −700 mV) at 25 °C. The EIS was recorded over a frequency range of $0.1-10^6$ Hz. The ac amplitude and the applied voltage were 10 mV and set −700 mV of the cells, respectively. The interfacial charge-transfer resistances and the electrochemical capacitances formed between interfaces were analyzed using the Z-View software (Solarton Analytical).

To investigate the electrochemical properties of bis-EDOT and Ru dye (Z-907) with and without illumination, cyclic voltammety measurements (CV) were carried out in a three-electrode measuring device in 0.1 M $LiClO_4$ acetonitrile solution, and a 1 cm^2 area of the FTO/TiO_2/dye or FTO served as the working electrode. A platinum foil and Ag/AgCl served as the counterelectrode, and reference electrode, respectively (BAS 100B/W electrochemical system). The film thicknesses of PEDOT were measured with a surface profilometer (Dektak 3 from Sloan Tech.).

3. Results and Discussion

3.1. Study of in Situ Photoelectropolymerization of PEDOT. In order to understand the photoelectrochemical polymerization mechanism used for the synthesis of PEDOT, we carried out basic characterization studies of separate solutions made of the monomer bis-EDOT and the TiO_2/Z-907 each in acetonitrile solvent. For comparison purposes the experiments were carried out under dark and illumination conditions. Figure 1 shows the corresponding cyclic voltammograms obtained for the monomer bis-EDOT and the TiO_2/Z-907 in acetonitrile. In

(16) Fukuri, N.; Saito, Y.; Kubo, W.; Senadeera, G. K. R.; Kitamura, T.; Wada, Y.; Yanagida, S. *J. Electrochem. Soc.* **2004**, *151*, A1745.
(17) Fukuri, N.; Masaki, N.; Kitamura, T.; Wada, Y.; Yanagida, S. *J. Phys. Chem. B* **2006**, *110*, 25251.
(18) Mozer, A. J.; Jiang, K. J.; Wada, Y.; Masaki, N.; Mori, S. N.; Yanagida, S. *Appl. Phys. Lett.* **2006**, *89*, 043509.
(19) Kiebooms, R.; Aleshin, A.; Hutchison, K.; Wudl, F. *J. Phys. Chem. B* **1997**, *101*, 11037.
(20) Li, C.; Imae, T. *Macromolecules* **2004**, *37*, 2411.
(21) Murayama, M.; Mori, T. *Thin Solid Films* **2006**, *509*, 123.

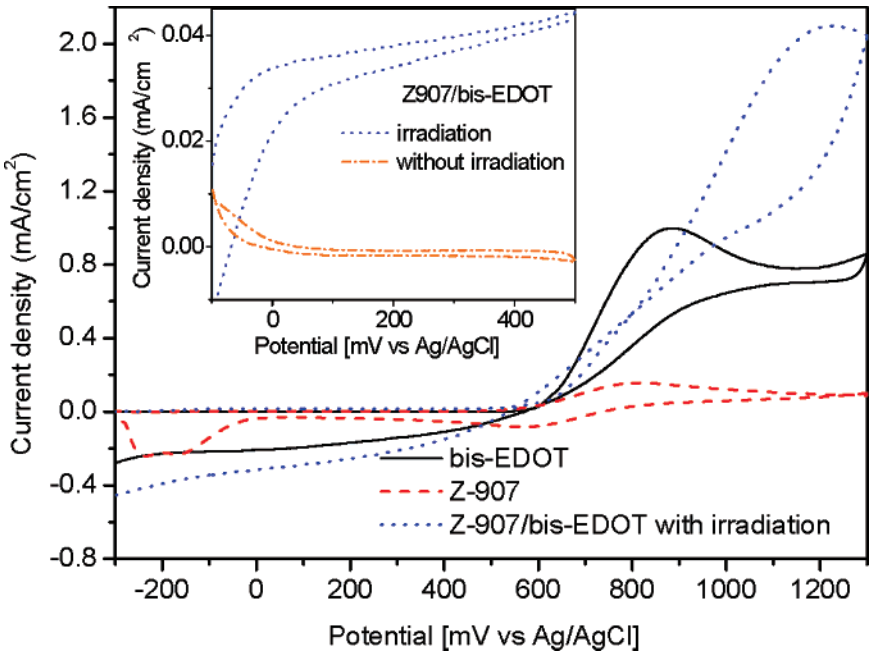

Figure 1. CV of bis-EDOT, Z-907, and Z-907/bis-EDOT with or without irradiation. The inset is the comparison of the irradiation effect on Z-907/bis-EDOT system. Supporting electrolyte: 0.1 M $LiClO_4$ in acetonitrile.

the dark, the onset of bis-EDOT oxidation potential is observed around 600 mV, while the onset oxidation potential for the Z-907 is observed around 500 mV. These results indicate that the electrochemical polymerization of bis-EDOT must be carried out at potentials above the oxidation limit for the Ru dye (Z-907) which could be a possible cause of dye degradation (overoxidation). Under illumination conditions, however, the Z-907/bis-EDOT shows an important current response in the whole voltage range, especially in the range between 0 and 500 mV. In order to analyze this effect, we examined the cyclic voltammograms in the voltage range between −100 and +500 mV (see inset of Figure 1) and observed respective increases in current from zero to 20−40 μA when shifting from the dark into illumination conditions, respectively.

It is obvious that the excited Ru dye molecules play a key role in the in situ photoelectropolymerization processes. The excited-state energy level of Z-907 can be extracted from the ground-state oxidation potential $E(Ru^{2+/3+})$ and its excitation energy E_{0-0} according to eq 1[22,23]

$$E^*(Ru^{2+/3+}) = E(Ru^{2+/3+}) - E_{0-0} \qquad (2)$$

Since the ground-state $E(Ru^{2+/3+})$ of Z-907 is 0.65 V vs Ag/AgCl while the E_{0-0} value was estimated to be 1.64 eV,[24] the excited state is around −0.99 V vs Ag/AgCl. Then the hole of the excited dye (0.65 V vs Ag/AgCl) will trigger the polymerization of bis-EDOT. The latter means that light creates positive and negative charges at the Z-907/TiO_2 interface, and this increases the conductivity over the interface to enhance the reactivity. Taking into consideration the configuration of our iodine-free ss-DSCs, the electrochemical window should be in the range of 0−0.5 V for the success of the in situ photoelectrochemical polymerization. Thus, we employ 0.2 V as our frequently optimized applied potential.

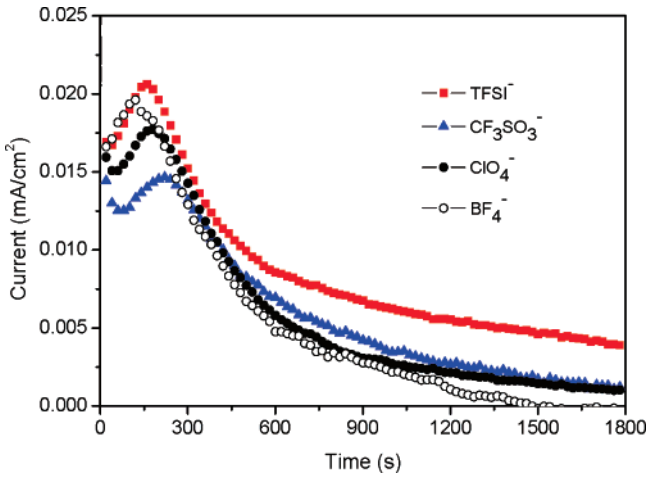

Figure 2. Current−time transient for 0.01 M bis-EDOT in situ photoelectropolymerization with different doping anions on FTO/TiO_2/Z-907 electrode. Applied potential 0.2 V vs Ag/AgCl.

The recorded current traces during the in situ photoelectrochemical polymerization of bis-EDOT using dye-coated TiO_2 films are shown in Figure 2. All current curves are similar; that is, they reach maximum within 100−200 s, and the current undergoes a drastic decrease to microampere level after an initial pulse. Such a curve shape is not representative of a steady potential to control polymerization. As discussed above, the excited Ru dye plays an important role in in situ photoelectropolymerization process. Once the dye is excited by illumination, the oxidation of bis-EDOT initiates, and PEDOT starts to form. Then the surface of the Z-907/TiO_2 electrode is slowly being covered by the PEDOT during photopolymerization, and a decrease of the amount of light reaching and activating the Z-907 dye is observed. As a result, the latter gives a weaker driving force capable of achieving photoelectrochemical polymerization of the bis-EDOT. The process continues until the

(22) Islam, A.; Sugihara, H.; Arakawa, H. *J. Photochem. Photobiol., A* **2003**, *158*, 131.
(23) Sauvé, G.; Cass, M. E.; Coia, G.; Doig, S. J.; Lauermann, I.; Pomykal, K. E.; Lewis, N. S. *J. Phys. Chem. B* **2000**, *104*, 6821.
(24) Wang, P.; Zakeeruddin, S. M.; Moser, J. E.; Grätzel, M. *J. Phys. Chem. B* **2003**, *107*, 13280.

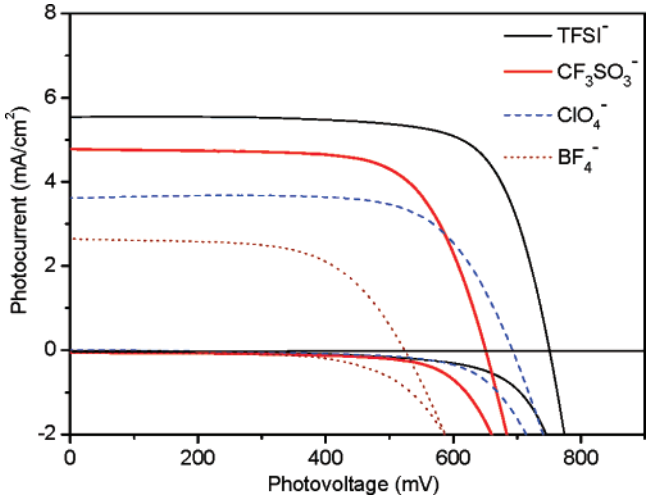

Figure 3. Current density vs voltage curves of iodine-free ss-DSCs using different photoelectrochemically deposited PEDOT hole conductors. TiO_2 layer thickness is 5.5 μm.

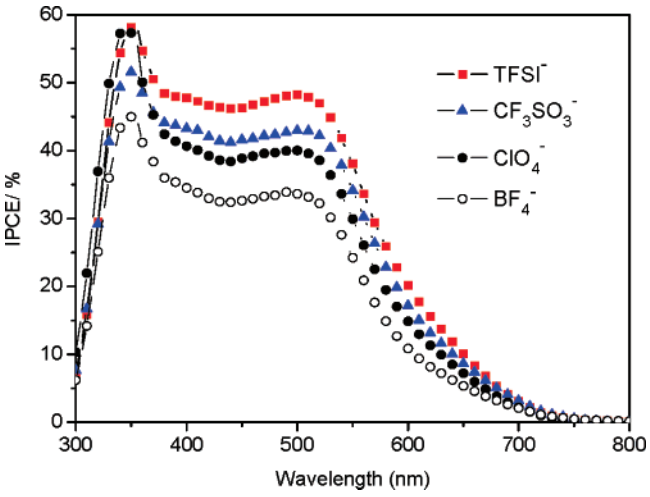

Figure 4. IPCE spectra of PEDOT/DSCs fabricated by different doping anions: $TFSI^-$ (square), $CF_3SO_3^-$ (triangle), ClO_4^- (solid circle), and BF_4^- (open square).

Table 1. Photovoltaic Properties of the Different Iodine-Free Solid-State PEDOT/DSCs

doping ions	V_{oc} (mV)	J_{sc} (mA/cm²)	FF	η (%)
ClO_4^-	690 ± 20	3.6 ± 0.3	0.72 ± 0.02	1.8 ± 0.1
$TFSI^-$	750 ± 50	5.3 ± 0.6	0.73 ± 0.02	2.85 ± 0.2
$CF_3SO_3^-$	635 ± 5	4.8 ± 0.4	0.71 ± 0.01	2.15 ± 0.1
BF_4^-	510 ± 20	2.8 ± 0.2	0.63 ± 0.02	0.9 ± 0.1

Z-907 dye is fully covered with PEDOT and the PEDOT completely blocks the light reaching the dye. At this moment the in situ photoelectropolymerization is terminated.

3.2. *I*−*V* Curves and IPCE Performance with Different Doping Anions. Complete iodine-free ss-DSCs were fabricated by using PEDOT as the hole-conducting material as described previously. Solar cell properties are strongly affected by the counteranion used during photoelectrochemical polymerization of PEDOT (see Scheme 1 for anions used). Figure 3 and Figure 4 show the I−V curves and the corresponding IPCE spectra of the iodine-free ss-DSCs, depending on the doping anion applied. For comparison purposes Table 1 shows detailed solar cell parameters obtained for each case. The best performance

Table 2. Relationship between Cells' Conversion Efficiency with the Conductivity of Different PEDOT Hole Conductors, the Obtained in Situ Photoelectropolymerization Charge, Series Resistance (R_s) and Shunt Resistance (R_{sh}) Values of the Devices

doping ions	charge of PEP (mC/cm²)	conductivity S/cm	R_s (Ω)	R_{sh} (kΩ)	η (%)
ClO_4^-	10.7	30	97.2	8.36	1.8 ± 0.1
$TFSI^-$	15.8	130	48.3	25.6	2.85 ± 0.2
$CF_3SO_3^-$	10.7	86	60.4	4.47	2.15 ± 0.1
BF_4^-	9.5	7.5	121	2.65	0.9 ± 0.1

(highest J_{sc} and V_{oc}) was observed for the iodine-free ss-DSC using PEDOT doped with $TFSI^-$ anion, showing a 2.85% solar cell conversion efficiency, the highest conversion efficiency reported thus far for an iodine-free ss-DSC based on PEDOT as the hole conductor. Following a descending order in performance is the PEDOT doped with $CF_3SO_3^-$ anion which shows 2.15% efficiency, 10% higher than that of the iodine-free ss-DSC using PEDOT doped with ClO_4^- anion with 1.8% efficiency. Finally, the lowest values were observed for iodine-free ss-DSC using PEDOT doped with BF_4^-, obtaining a 0.9% conversion efficiency. Comparison between *I*−*V* curves in the dark shows that photocurrent response and IPCE values follow the same descending trend: the best performance and a 50% IPCE value was obtained for the iodine-free ss-DSC using PEDOT doped with $TFSI^-$. The former is comparable with results obtained for ionic liquid-based DSCs. Our results show that $TFSI^-$ presents superior performance as a doping anion for PEDOT hole conductor than the one observed with $CF_3SO_3^-$ or ClO_4^-. This could be explained in terms of charge delocalization; that is, the application of a softer anion seems to have a better effect on PEDOT-based DSC performance. Detailed discussion will be carried out by the impedance spectroscopy analysis. In addition, the dark current of the cell fabricated by $TFSI^-$ anion was improved to the greatest extent when compared with the others.

3.3. Comparison of the Conductivity of PEDOT Hole Conductor. Properties of conducting polymers such as conductivity depend a great extent on experimental parameters used during the synthesis, such as the doping ion, the solvent type, or the preparation methods. Table 2 summarizes the values obtained for these sets of experiments such as photoelectropolymerization charge (mC/cm²), conductivity (σ), series resistance (R_s), shunt resistance (R_{sh}), as well as the corresponding conversion efficiency obtained for each iodine-free ss-DSC. We can observed that, except for the PEDOT/$TFSI^-$ system, the charge consumed for polymerization is independent of the counteranion used, about 10 mC/cm². In order to analyze these results we (a) neglect the thickness of the porous dye/TiO_2 films which is, in all cases, constant; (b) consider that the PEDOT thickness is proportional to the photoelectropolymerization charge, which is approximately 1.7 μm/100 mC; and (c) assume that all PEDOT layers have the same thickness (around 200 nm). Thus, the conductivity observed for the PEDOT layer is directly dependent on the doping anion, decreasing thusly $TFSI^-$ > $CF_3SO_3^-$ > ClO_4^- > BF_4^-, as is shown in Table 2.

Taking into account that the polymerization charges of the $CF_3SO_3^-$, ClO_4^-, and BF_4^- are comparable, we believe that the doping anions play a key role in the conductivity of the PEDOT hole conductor. Partially due to the fact that the total polymerization charge of $TFSI^-$ is increased about 50% higher

than the other three systems, the PEDOT/TFSI$^-$ shows the highest conductivity among the investigated systems. The sequence is consistent with that of the solar cells' performances. That is, PEDOT/TFSI$^-$ shows the highest conductivity, which is reflected by its best performance in iodine-free ss-DSCs. In addition, such evidence is supported by Djellab et al.,[25] who found that the conductivity by doping TFSI$^-$ anion is triple that of doping ClO_4^- in the case of poly(3-methylthiophene).

Without considering the influence of Li^+, we discuss the effect of anions in the conductivity of PEDOT. Previous studies[26] indicate that TFSI$^-$ has highly delocalized charge density with relatively large ionic radius, which resulted in smaller ion association and in the formation of triple ions, $(Li_2N(CF_3SO_2)_2^+$ and $Li(N(CF_3SO_2)_2)_2^-)$, in acetonitrile. Furthermore, the existence of charge-delocalized polarons, bipolarons, and polaronic clusters are related to the soft−soft attractions with the doped anions. Therefore, the more charge-delocalized TFSI$^-$ anion will induce preferred stacking through the transverse PEDOT ring, resulting in excellent conductivity. It seems that the cells' performances show a linear dependence on log σ (see Supporting Information). Here we simply discuss the difference between the PEDOT and spiro-OMeTAD system. The conductivity of PEDOT is on the order of 5−6 times higher than that of spiro-OMeTAD.[8] In general, the conductivity is composed of ionic conductivity and electronic conductivity. In the spiro-MeOTAD system, the addition of LiTFSI[8] can greatly improve ionic conductivity. However, in our PEDOT conductive polymer system, electronic conductivity is the main part, which will be determined by doping anions.

Moreover, PEDOT/TFSI$^-$ shows the lowest R_s and highest R_{sh} whereas PEDOT/BF_4^- shows the highest R_s with the lowest R_{sh} (see Table 2). It is well-known that R_s arises from the resistance of the cell material to current flow and from resistive contacts, and that R_{sh} arises from leakage of current through the cell. Thus, it is not surprising that the application of the PEDOT layer with higher conductivity (that is the PEDOT/TFSI$^-$ system) presents the lowest series resistance and an improved hole conductivity among all these iodine-free ss-DSCs. On the other hand, the balance of the electron- and hole-transporting properties will increase the hole-transporting or hole-injection efficiency in the PEDOT/TFSI$^-$ system, resulting in an improvement of the photocurrent of the device. In addition, R_{sh} of PEDOT/TFSI$^-$ shows the highest value. This indicates that the electron leakage current from the dye molecules to the PEDOT hole conductor is well suppressed, which is also consistent with the low value observed for dark current as shown in Figure 3.

3.4. Impedance of PEDOT/DSCs. Figure 5 shows Cole−Cole plots of the DSCs and a fitted Bode phase angle (Figure 5b) of experiments carried out under dark conditions at minus 700 mV. The results are based on the equivalent circuits shown as the inset in Figure 5a. The equivalent circuits of DSCs can be represented by two *RC* circuits in parallel, in good agreement with previously published works.[27,28] The observed *R* and *C* values obtained after fitting are presented in Table 3. Two semicircles were observed in the measured frequency range of

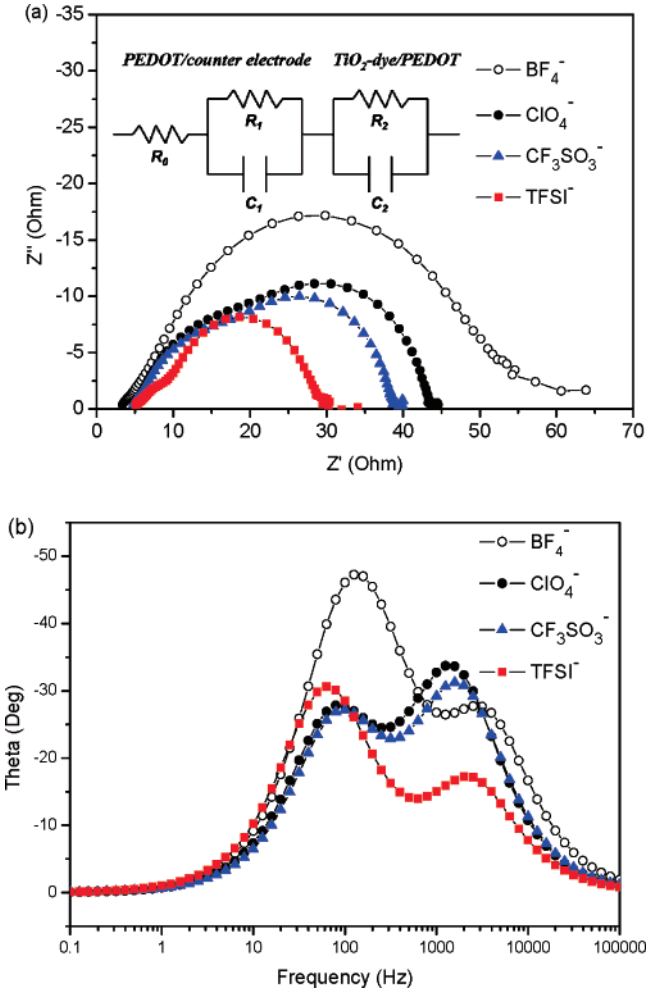

Figure 5. Electrochemical impedance spectra of iodine-free ss-DSCs with different doping anions: TFSI$^-$ (square), $CF_3SO_3^-$ (triangle), ClO_4^- (solid circle), and BF_4^- (open square). (a) Nyquist plots; (b) fitted Bode phase plots.

Table 3. Parameters Obtained by Fitting the Impedance Spectra of PEDOT/DSCs Shown in Figure 5a Using the Equivalent Circuit

	R_0 Ω cm^2	R_1 Ω cm^2	C_1 F cm^{-2}	R_2 Ω cm^2	C_2 F cm^{-2}
BF_4^-	3.88	4.45	1.51×10^{-5}	45.0	6.80×10^{-5}
ClO_4^-	5.61	11.1	1.64×10^{-5}	25.8	1.31×10^{-4}
TFSI$^-$	5.72	4.02	2.10×10^{-5}	19.7	2.23×10^{-4}
$CF_3SO_3^-$	5.59	9.63	1.56×10^{-5}	22.8	1.31×10^{-4}

10^{-1} to 10^5 Hz for all PEDOT solid-state solar cells. According to the previous works,[28,17] the semicircles in the frequency regions 10^3−10^5 and 1−10^3 Hz correspond to charge-transfer processes occurring at the Au/PEDOT and the FTO−TiO_2/dye/PEDOT interface. Our results show that the first semicircle (R_1) is larger than that obtained from using organic or ionic liquid electrolytes, which means that the charge transport at the Au/PEDOT hole conductor interface is more difficult in our system than in a DSC using liquid- or ionic liquid-based systems.

We can also observe from Table 3 that the PEDOT/BF_4^- system and the PEDOT/TFSI$^-$ system show similar R_1 values, indicating a good contact between PEDOT and the Au metal electrode. Nevertheless, the PEDOT/BF_4^- system shows the worst conversion efficiency of all, indicating that charge transfer (especially the fluent hole-transporting ability based on PEDOT) between the TiO_2/dye and the hole-transport PEDOT layer is

(25) Djellab, H.; Armand, M.; Delabouglise, D. *Synth. Met.* **1995**, *74*, 223.
(26) Salomon, M. *J. Solution Chem.* **1993**, *22*, 715.
(27) Longo, C.; Nogueira, A. F.; Paoli, M.-A. D. *J. Phys. Chem. B* **2002**, *106*, 5925.
(28) Han, L.; Koide, N.; Chiba, Y.; Mitate, T. *Appl. Phys. Lett.* **2004**, *84*, 2433.

very essential. The latter is reflected in the different values of R_2 obtained, being the PEDOT/BF_4^- the system with the highest R_2 value, while PEDOT/$TFSI^-$ shows the lowest one, in good agreement with the reversed order observed for the conversion efficiency. The latter results indicate that the PEDOT/$TFSI^-$ exhibits an excellent charge transfer between PEDOT/$TFSI^-$ and the TiO_2/dye due to its good hole-conducting properties. Although the contact between PEDOT and the Au counterelectrode has great influence on the iodine-free ss-DSC performance, our results show that the balance between hole mobility and electron conductivity of PEDOT as well as the complete filling of the porous dye/TiO_2 electrode by PEDOT are key issues for an efficient solar cell performance.

On the other hand, according to our previous study,[17] the ratio of the volume occupied with PEDOT in mesoporous TiO_2 was given ca. 20%, which means that there is still a lot of vacant space and especially those dye molecules without PEDOT covered would be electron recombination sites once the devices have higher J_{sc}. We would expect that large pore sized TiO_2 would be helpful for the PEDOT filling. This is another possible way to further optimize the device performance. In addition, according to the recent studies by Thelakkat et al.[29,30] and Huang et al.,[31] the filling effect on the different pores of TiO_2 is important in the case of solid-state DSC and viscous ionic liquid-based DSC. In our system, we need to think about the pore structure of TiO_2 and the growth rate of PEDOT during the photoelectropolymerization processes.

Finally, we would like to comment on the electron lifetime (τ_e) in the TiO_2 film. This value can be obtained from the characteristic frequency angle (ω_{mid}) of the midfrequency peak (f_{mid}) of the bode-phase plots. Thus, using the latter together with the equation of $\tau_e = 1/\omega_{mid} = 1/2\pi f_{mid}$[32,33] we are able to extract information on electron lifetime. We can observed that PEDOT/BF_4^- exhibits the maximum f_{mid} of 125.9 Hz, followed by PEDOT/ClO_4^- and PEDOT/$CF_3SO_3^-$ with moderate values around 79.4 and 100.0 Hz, respectively, and finally PEDOT/$TFSI^-$ which shows the minimum f_{mid} of 63.1 Hz. These results show that PEDOT/$TFSI^-$ presents the longest τ_e of 2.5 ms which is increased by a factor of 2 when compared with PEDOT/BF_4^-. These results demonstrate that the use of PEDOT/$TFSI^-$ in iodine-free ss-DSCs decreases the charge recombination between injected electrons and oxidized PEDOT and explains the large output voltage, V_{oc}, obtained for these devices.

4. Conclusions

Here we present an effective way to tune the conductivity of PEDOT hole conductor by a careful selection of different doping anions. These doping anions present a direct effect on the conversion efficiency of iodine-free ss-DSCs. The use of $TFSI^-$ anion presented the best results, obtaining the lowest R_s and highest R_{sh} values which are the best conditions for an efficient iodine-free ss-DSC. Furthermore, analyses by EIS demonstrated that PEDOT/$TFSI^-$ exhibits an excellent charge transfer between PEDOT/$TFSI^-$ and TiO_2/dye for the unidirectional electron flow required in an iodine-free ss-DSC. The optimization of these parameters allowed us to obtain an iodine-free ss-DSC with J_{sc} of 5.3 mA/cm^2, V_{oc} of 750 mV, and a conversion efficiency of 2.85% which is the highest efficiency obtained thus far for an iodine-free ss-DSC using PEDOT as hole conductor. Further efforts such as designing and synthesizing novel hybrid Ru dyes, preparing more porous TiO_2 films, and optimizing hole conductors filling into porous TiO_2 films are in progress.

Acknowledgment. This research was supported by the New Energy and Industrial Technology Development Organization (NEDO) under the Ministry of Economy, Trade and Industry.

Supporting Information Available: The dependence of conversion efficiency with conductivity of PEDOT hole conductor. This material is available free of charge via the Internet at http://pubs.acs.org.

JA075704O

(29) Schmidt-Mende, L.; Grätzel, M. *Thin Solid Films* **2006**, *500*, 296.
(30) Karthikeyan, C. S.; Thelakkat, M.; Willert-Porada, M. *Thin Solid Films* **2006**, *511−512*, 187.
(31) Chen, Z. G.; Yang, H.; Tang, Y. W.; Li, F. Y.; Yi, T.; Huang, C. H. *J. Power Sources* **2007**, *171*, 990.
(32) Kern, R.; Sastrawan, R.; Ferber, J.; Stangl, R.; Luther, *J. Electrochim. Acta* **2002**, *47*, 4213.
(33) Wang, N.; Lin, H.; Li, J. B.; Li, X. *Appl. Phys. Lett.* **2006**, *89*, 194104.